

SU(3) orbital Kondo effect with ultracold atoms

Yusuke Nishida

Department of Physics, Tokyo Institute of Technology, Ookayama, Meguro, Tokyo 152-8551, Japan

(Dated: August 2013)

We propose a simple but novel scheme to realize the Kondo effect with ultracold atoms. Our system consists of a Fermi sea of spinless fermions interacting with an impurity atom of different species which is confined by an isotropic potential. The interspecies attraction can be tuned with an s -wave Feshbach resonance so that the impurity atom and a spinless fermion form a bound dimer that occupies a threefold-degenerate p orbital of the confinement potential. Many-body scatterings of this dimer and surrounding spinless fermions occur with exchanging their angular momenta and thus exhibit the SU(3) orbital Kondo effect. The associated Kondo temperature has a universal leading exponent given by $T_K \propto \exp[-\pi/(3a_p k_F^3)]$ that depends only on an effective p -wave scattering volume a_p and a Fermi wave vector k_F . We also elucidate a Kondo singlet formation at zero temperature and an anisotropic interdimer interaction mediated by surrounding spinless fermions. The Kondo effect thus realized in ultracold atom experiments may be observed as an increasing atom loss by lowering the temperature or with radio-frequency spectroscopy. Our scheme and its extension to a dense Kondo lattice will be useful to develop new insights into yet unresolved aspects of Kondo physics.

PACS numbers: 67.85.Pq, 72.10.Fk, 72.15.Qm, 75.20.Hr

Introduction

The Kondo effect plays fundamental roles in a wide range of condensed matter physics. The Kondo effect arises from coherent many-body scatterings between a localized magnetic impurity and a surrounding Fermi sea of itinerant electrons with the exchange of their spins [1, 2]. While the Kondo effect was originally discovered in explaining an anomalous electrical resistivity minimum in dilute magnetic alloys [3], it has been observed also in artificial nanosystems such as quantum dots [4–6], carbon nanotubes [7, 8], and individual molecules [9, 10]. Furthermore, the role of the spin can be replaced by other degrees of freedom such as an orbital quantum number [11], which leads to the orbital Kondo effect [12, 13]. In spite of the fact that the Kondo effect is well known and widely studied, there are yet unresolved issues, for example, regarding the formation of the Kondo screening cloud and its dynamics [14].

Ultracold atoms may be useful to develop new insights into this old but still actively studied phenomenon. This is because a highly tunable clean system that is suitable to study a desired phenomenon can be created at will by using optical lattices and Feshbach resonances. This scheme called “quantum simulation” has been successfully implemented to study a rich variety of strongly correlated many-body phenomena [15]. Regarding the realization of the Kondo effect, essential ingredients are (i) degenerate degrees of freedom that can be exchanged between a localized impurity and surrounding fermions and (ii) a mechanism that suppresses a double occupancy of the localized state. While both ingredients are naturally incorporated in condensed matter systems by the spin and Coulomb repulsion of charged electrons, they are in general difficult to achieve simultaneously with

neutral atoms. Accordingly, previously proposed theoretical schemes to realize the Kondo effect with ultracold atoms [16–21] are somewhat involved and demanding and thus the experimental realization is still lacking.

In this Letter, we propose a simple but novel scheme to realize the Kondo effect with ultracold atoms. Our system consists of a Fermi sea of spinless fermions of species A interacting with an impurity atom of different species B which is loaded into a ground state of an isotropic potential $V_B(r)$:

$$\begin{aligned} H = & \int d\mathbf{r} \Psi_A^\dagger(\mathbf{r}) \left[-\frac{\hbar^2 \nabla^2}{2m_A} - E_F \right] \Psi_A(\mathbf{r}) \\ & + \int d\mathbf{r} \Psi_B^\dagger(\mathbf{r}) \left[-\frac{\hbar^2 \nabla^2}{2m_B} + V_B(r) \right] \Psi_B(\mathbf{r}) \\ & + U_{AB} \int d\mathbf{r} \Psi_A^\dagger(\mathbf{r}) \Psi_B^\dagger(\mathbf{r}) \Psi_B(\mathbf{r}) \Psi_A(\mathbf{r}). \quad (1) \end{aligned}$$

By tuning the interspecies attraction $U_{AB} < 0$ with an s -wave Feshbach resonance, the impurity atom and a spinless fermion can form a bound dimer that occupies a threefold-degenerate p orbital of the confinement potential [22]. It is important to note that the impurity atom cannot bind two spinless fermions simultaneously because of the Pauli exclusion principle. Many-body scatterings of this dimer and surrounding spinless fermions occur with exchanging their angular momenta and thus exhibit the SU(3) orbital Kondo effect. In what follows, we give a detailed account of how the Kondo effect emerges in our simple system and elucidate its fundamental properties such as a universal leading exponent of the Kondo temperature, a Kondo singlet formation at zero temperature, an anisotropic interdimer interaction mediated by surrounding spinless fermions, and possible experimental signatures. Below we denote a kinetic energy of spinless

fermions by $\epsilon_{\mathbf{k}} = \hbar^2 \mathbf{k}^2 / (2m_A)$ and set $\hbar = 1$.

Few-body scattering and effective theories

Before working on the many-body Kondo effect, we first need to elucidate the few-body scattering properties of our system (1). A two-body scattering of an A atom with a confined B atom was studied in Ref. [22]. There it was found that by tuning the interspecies attraction with an s -wave Feshbach resonance, a p -wave scattering resonance can be induced. An intuitive picture for this seemingly counterintuitive result is actually simple [22–24]: A Feshbach molecule formed by the A and B atoms is subject to the confinement potential and thus its center-of-mass energy is quantized. By decreasing its internal energy with the interspecies attraction, the total energy of the AB molecule in the p orbital intersects the scattering threshold of the A and B atoms. At this point, the p -wave scattering resonance is induced and low-energy physics in its vicinity is described by a two-channel Hamiltonian:

$$H_{2\text{ch}} = \int \frac{d\mathbf{k}}{(2\pi)^3} \epsilon_{\mathbf{k}} \psi_A^\dagger(\mathbf{k}) \psi_A(\mathbf{k}) + \epsilon_{AB} \sum_{\mu} \phi_{\mu}^\dagger \phi_{\mu} + g \sum_{\mu} \int^{\Lambda} \frac{d\mathbf{k}}{(2\pi)^3} k_{\mu} \left[\psi_A^\dagger(\mathbf{k}) \psi_B^\dagger \phi_{\mu} + \phi_{\mu}^\dagger \psi_B \psi_A(\mathbf{k}) \right]. \quad (2)$$

Here ψ_B^\dagger is a creation operator of the impurity B atom in the ground state of the isotropic potential whose energy is chosen to be zero, while ϕ_{μ}^\dagger is that of the AB molecule in one of the threefold-degenerate p orbitals labeled by $\mu = x, y, z$. Because of the angular momentum conservation, this AB molecule can couple with the impurity B atom and an A atom only with the same orbital quantum number μ , which is created by $\psi_{A\mu}^\dagger(k) \equiv \int d\Omega \hat{k}_{\mu} \psi_A^\dagger(\mathbf{k})$. The particle number operators of the localized B atom and AB molecule are constrained by

$$N_B = \psi_B^\dagger \psi_B + \sum_{\mu} \phi_{\mu}^\dagger \phi_{\mu} = 1 \quad (3)$$

because only one B atom is confined. Therefore, the above two-channel Hamiltonian corresponds to the infinite- U Anderson impurity model in the slave-particle representation [25, 26]. We also note that the same Hamiltonian (2) can be realized with an interspecies p -wave Feshbach resonance, which is referred to as a p -wave Fano-Anderson model in Ref. [27].

The low-energy effective description (2) is valid well below a ultraviolet cutoff $\Lambda \sim \sqrt{m_B \omega_{\text{ho}}}$, which is a momentum scale set by an inverse characteristic extent of the confined B atom. The remaining two couplings ϵ_{AB} and g can be related to physical parameters to characterize

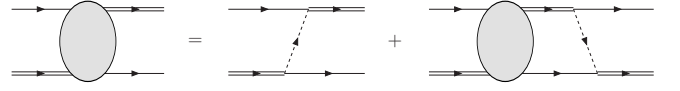


FIG. 1. Atom-dimer scattering \mathcal{T} matrix in the vacuum represented by the blob. Solid, dotted, and double lines correspond to Green's functions of the A atom, B atom, and AB molecule, respectively.

a low-energy p -wave scattering, namely, a scattering volume a_p and an effective momentum r_p . By matching the two-body scattering amplitude computed from Eq. (2) with the standard formula, we find $-\frac{\epsilon_{AB}}{g^2} + \frac{m_A \Lambda^3}{9\pi^2} = \frac{m_A}{6\pi} \frac{1}{a_p}$ and $\frac{1}{2m_A g^2} + \frac{m_A \Lambda}{3\pi^2} = -\frac{m_A}{6\pi} \frac{r_p}{2} > 0$, respectively. Information on $V_B(r)$ and U_{AB} in the original Hamiltonian (1) is now encoded into a_p and r_p , which have been determined as functions of an s -wave scattering length in the case of a harmonic potential $V_B(r) = m_B \omega_{\text{ho}}^2 r^2 / 2$ [22]. (It is worthwhile to note that, unlike an s -wave scattering resonance, the cutoff Λ cannot be sent to infinite with a_p and r_p fixed because $|r_p| > 4\Lambda/\pi$.) By using a_p and r_p , the renormalized Green's function of the AB molecule at energy E is expressed as $g^2 \langle T \phi_{\nu} \phi_{\mu}^\dagger \rangle = i \delta_{\mu\nu} \mathcal{D}(E)$, where

$$\mathcal{D}(E) = \frac{6\pi}{m_A} \frac{1}{\frac{1}{a_p} - \frac{|r_p|}{2} \kappa^2 + \frac{2}{\pi} \kappa^3 \arctan\left(\frac{\Lambda}{\kappa}\right)} \quad (4)$$

with $\kappa \equiv \sqrt{-2m_A E - i0^+}$. When the effective p -wave scattering volume a_p is positive, Eq. (4) develops a pole at $E = \mathcal{E} < 0$ with a corresponding residue \mathcal{Z} . This means the existence of threefold-degenerate bound dimer states that carry an orbital angular momentum $\ell = 1$. Because of the constraint (3), only one of them can be occupied at one time.

We then study a scattering of this bound dimer with another A atom which is now a three-body problem. The corresponding scattering \mathcal{T} matrix at energy E solves an integral equation depicted in Fig. 1:

$$\mathcal{T}_{\mu\nu}(P; Q) = -\frac{q_{\mu} p_{\nu} \mathcal{Z}}{E - p_0 - q_0 + i0^+} - \sum_{\lambda} \int^{\Lambda} \frac{d\mathbf{k}}{(2\pi)^3} \mathcal{T}_{\mu\lambda}(P; K) \frac{q_{\lambda} k_{\nu} \mathcal{D}(E - k_0)}{E - k_0 - q_0 + i0^+} \Big|_{k_0 = \epsilon_{\mathbf{k}}} \quad (5)$$

Here $P = (p_0, \mathbf{p})$ [$Q = (q_0, \mathbf{q})$] is a set of energy and momentum of the incoming (outgoing) A atom and μ (ν) labels a p orbital that is initially (finally) occupied by the bound dimer. The atom-dimer scattering \mathcal{T} matrix at their scattering threshold is obtained from $\mathcal{T}_{\mu\nu}(P; Q)$ by setting $p_0 = q_0 = 0$ and $E = \mathcal{E}$. The resulting quantity $t_{\mu\nu}(\mathbf{p}; \mathbf{q}) \equiv \mathcal{T}_{\mu\nu}(0, \mathbf{p}; 0, \mathbf{q})|_{E=\mathcal{E}}$ is in general cutoff dependent and thus not universal, but we find that it becomes universal in the vicinity of the p -wave scattering

resonance:

$$\lim_{a_p \rightarrow +\infty} t_{\mu\nu}(\mathbf{p}; \mathbf{q}) = \frac{6\pi a_p}{m_A} q_\mu p_\nu \quad (6)$$

with $g < \infty$ and Λ fixed. Technically, this is because the source term in Eq. (5) dominates over the integral term, which means that the Born approximation turns out to be exact for this particular quantity sufficiently close to the resonance. A similar universality was found in the corresponding atom-dimer scattering problem without the confinement potential [28]. We also confirmed by numerically solving the integral equation (5) that three-body bound states do not exist in the same limit as in Eq. (6); i.e., the impurity atom cannot bind two spinless fermions simultaneously.

We finally arrive at a stage to write down an effective Hamiltonian that describes the above low-energy scattering of an A atom with a bound dimer in the vicinity of the p -wave scattering resonance $a_p \Lambda^3 \gg 1$:

$$H_{\text{ad}} = \int \frac{d\mathbf{k}}{(2\pi)^3} \epsilon_{\mathbf{k}} \psi_A^\dagger(\mathbf{k}) \psi_A(\mathbf{k}) + \sum_{\mu, \nu} \int \int^{\Lambda'} \frac{d\mathbf{p} d\mathbf{q}}{(2\pi)^6} \psi_A^\dagger(\mathbf{q}) \psi_A(\mathbf{p}) [v q_\mu p_\nu + v' \delta_{\mu\nu} \mathbf{q} \cdot \mathbf{p}] \phi_\nu^\dagger \phi_\mu. \quad (7)$$

Here the two couplings $v = \frac{6\pi a_p}{m_A} / [1 - (\frac{2a_p \Lambda^3}{3\pi})^2]$ and $v' = \frac{2a_p \Lambda^3}{3\pi} v$ are determined so that the zero-energy atom-dimer scattering \mathcal{T} matrix $t_{\mu\nu}(\mathbf{p}; \mathbf{q})$ obtained in Eq. (6) is correctly reproduced from Eq. (7). This low-energy effective description is valid well below the new ultraviolet cutoff $\Lambda' \sim 1/\sqrt{a_p |r_p|}$, which is now a momentum scale set by an inverse characteristic extent of the bound dimer. The atom-dimer Hamiltonian (7) reduced from Eq. (2) corresponds to the Kondo or Coqblin-Schrieffer model reduced from the Anderson impurity model [29, 30] and thus serves as a basis for the many-body Kondo effect.

Many-body physics and the Kondo effect

We are now prepared to work on the Kondo effect. We apply the atom-dimer Hamiltonian (7) to a many-body system of spinless fermions with a Fermi energy $E_F \equiv k_F^2/2m_A \equiv k_B T_F$ at a temperature T and study their scatterings with the localized dimer. We consider that the incoming (outgoing) fermion has a momentum $\mathbf{p} = k_F \hat{\mathbf{p}}$ ($\mathbf{q} = k_F \hat{\mathbf{q}}$) and the localized dimer initially (finally) occupies a p orbital labeled by μ (ν) and compute the corresponding scattering \mathcal{T} matrix $t_{\mu\nu}(\mathbf{p}; \mathbf{q})$ in a perturbative expansion over $a_p k_F^3$, $a_p k_F^2 \Lambda' \ll 1$ assuming a dilute system. The leading $O(a_p)$ term is simply the one obtained in Eq. (6) and thus does not involve the many-body effect. There are two distinct contributions

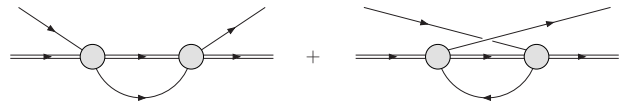


FIG. 2. Subleading contributions to the atom-dimer scattering \mathcal{T} matrix in the presence of a Fermi sea of spinless fermions. See Fig. 1 for the meanings of the symbols.

at subleading $O(a_p^2)$ depending on whether the intermediate scattering state is a particle or a hole, which is depicted by the left or right diagram in Fig. 2, respectively. By summing all contributions up to $O(a_p^2)$, the zero-energy atom-dimer scattering \mathcal{T} matrix in the low-temperature limit $T \ll T_F$ is found to be

$$\text{Re } t_{\mu\nu}(\mathbf{p}; \mathbf{q}) = \left(q_\mu p_\nu - \frac{\delta_{\mu\nu}}{3} \mathbf{q} \cdot \mathbf{p} \right) v(T) + \frac{\delta_{\mu\nu}}{3} \mathbf{q} \cdot \mathbf{p} \left(v_0 - v_0^2 \frac{m_A k_F^2}{\pi^2} \Lambda' \right) + O(a_p^3), \quad (8)$$

where $v_0 = 6\pi a_p/m_A > 0$ is the atom-dimer coupling in the vacuum [see Eq. (6)].

The first (second) term in Eq. (8) corresponds to a scattering process in which orbital quantum numbers are (not) exchanged between the spinless fermion and the localized dimer. While the second term is temperature independent, the first term depends on the temperature through

$$v(T) = v_0 + v_0^2 \frac{m_A k_F^3}{2\pi^2} \left[\ln \left(\frac{T_F}{T} \right) + \text{const} \right] + O(a_p^3). \quad (9)$$

This effective atom-dimer coupling exhibits the logarithmic growth by lowering the temperature which is the hallmark of the Kondo effect [3]. In particular, this is an SU(3) orbital Kondo effect because our low-energy effective Hamiltonian (2) or (7) is invariant under an SU(3) rotation of p -orbital indices of ϕ_μ and $\psi_{A\mu}(k)$. Furthermore, the leading logarithmic singularities can be summed up to all orders with the aid of the renormalization group equation: $\frac{dv(T)}{d \ln(T_F/T)} = \frac{m_A k_F^3}{2\pi^2} v^2(T)$, which is solved by $v(T) \simeq v_0 / [1 - v_0 \frac{m_A k_F^3}{2\pi^2} \ln(\frac{T_F}{T})]$. This renormalized effective coupling diverges at a Kondo temperature given by

$$T_K \propto T_F \exp \left(-\frac{\pi}{3a_p k_F^3} \right). \quad (10)$$

This expression is valid in the vicinity of the p -wave scattering resonance $a_p \Lambda^3 \gg 1$ for a sufficiently dilute system $a_p k_F^3$, $a_p |r_p| k_F^2 \ll 1$. Remarkably, we find that the Kondo temperature has a universal leading exponent that depends on details of the original Hamiltonian (1) only through the effective p -wave scattering volume a_p and the Fermi wave vector k_F .

The rate at which spinless fermions on the Fermi surface are scattered by localized dimers with a density n_d is obtained from the standard formula as

$$\begin{aligned} \frac{1}{\tau_{\text{ad}}} &= \frac{n_d}{3} \sum_{\mu,\nu} \int \frac{d\mathbf{q}}{(2\pi)^3} 2\pi \delta(\epsilon_{\mathbf{p}} - \epsilon_{\mathbf{q}}) |t_{\mu\nu}(\mathbf{p}; \mathbf{q})|^2 \\ &= \frac{8m_A n_d k_F^5}{27\pi} v^2(T) + \text{const}, \end{aligned} \quad (11)$$

which grows logarithmically according to Eq. (9). An atom-dimer scattering in ultracold atom experiments typically leads to a loss of atoms because the dimer can decay into a deeper bound state [31, 32] or a lower s orbital of the confinement potential in our scheme. Therefore, the logarithmic growth of the atom-dimer scattering rate (11) caused by the Kondo effect may be observed as an increasing atom loss by lowering the temperature, which is a direct analog of the celebrated increasing electrical resistivity in dilute magnetic alloys [33].

The divergence of the effective atom-dimer coupling (9) means the breakdown of the perturbation theory below the Kondo temperature $T \lesssim T_K$. Here the localized dimer interacts so strongly with surrounding spinless fermions that its angular momentum is effectively screened by the so-called Kondo screening cloud. Accordingly, the ground state becomes a singlet state instead of a naively expected triplet state. This nonperturbative physics can be captured by the following variational wave functions corresponding to the nondegenerate singlet state:

$$\begin{aligned} |s\rangle &= \left[\alpha \psi_B^\dagger + \sum_{\mu} \int^{k_F} \frac{d\mathbf{p}}{(2\pi)^3} \beta_{\mu}(\mathbf{p}) \phi_{\mu}^\dagger \psi_A(\mathbf{p}) \right. \\ &\quad \left. + \int^{k_F} \frac{d\mathbf{p}}{(2\pi)^3} \int_{k_F} \frac{d\mathbf{q}}{(2\pi)^3} \gamma(\mathbf{p}, \mathbf{q}) \psi_B^\dagger \psi_A^\dagger(\mathbf{q}) \psi_A(\mathbf{p}) \right] |\text{FS}\rangle \end{aligned} \quad (12)$$

and the threefold-degenerate triplet state ($\mu = x, y, z$):

$$|t\rangle_{\mu} = \left[\bar{\alpha} \phi_{\mu}^\dagger + \int_{k_F} \frac{d\mathbf{q}}{(2\pi)^3} \bar{\beta}_{\mu}(\mathbf{q}) \psi_B^\dagger \psi_A^\dagger(\mathbf{q}) \right] |\text{FS}\rangle, \quad (13)$$

where $|\text{FS}\rangle$ represents the Fermi sea of A atoms. The singlet state consists of a localized B atom dressed by a particle-hole excitation of A atoms which hybridizes with an AB molecule by absorbing an A atom from the Fermi sea. On the other hand, the triplet state consists of a localized AB molecule which hybridizes with a B atom by emitting an A atom to the Fermi sea. These two states have the same particle number $N_B = 1$ in compliance with the constraint (3) but have different orbital angular momenta, $\ell = 0$ and 1, respectively.

By minimizing the expectation values of the two-channel Hamiltonian (2) with respect to the variational parameters in Eqs. (12) and (13), we find that the energies of the singlet state E_s and the triplet state E_t apart

from the energy of the Fermi sea solve $G^{-1}(E_s) = 0$ and $D^{-1}(E_t + E_F) = 0$, respectively, where

$$D^{-1}(E) = \mathcal{D}^{-1}(E) + \frac{1}{3} \int \frac{d\mathbf{q}}{(2\pi)^3} \frac{q^2 \theta(k_F - q)}{E - \epsilon_{\mathbf{q}}} \quad (14)$$

is the inverse Green's function of the AB molecule and

$$G^{-1}(E) = E - \int \frac{d\mathbf{p}}{(2\pi)^3} p^2 \theta(k_F - p) D(E + \epsilon_{\mathbf{p}}) \quad (15)$$

is that of the B atom in the presence of the Fermi sea of A atoms. In the resonance and dilute limits $a_p k_F^3, a_p |r_p| k_F^2 \ll 1 \ll a_p \Lambda^3$ considered above [see below Eq. (10)], the energy of the triplet state approaches that of the bound dimer $E_t = -E_F - \frac{1}{m_A a_p |r_p|}$. Although this triplet state is already deeply bound with respect to the Fermi energy, the singlet state has an even lower energy given by

$$\begin{aligned} E_s &= E_t - E_F \exp\left(-\frac{\pi}{3a_p k_F^3} - \frac{\pi|r_p|}{6k_F} - \frac{8-6\ln 2}{3}\right) \\ &\simeq E_t - k_B T_K, \end{aligned} \quad (16)$$

where the same universal leading exponent as the Kondo temperature (10) appears in the binding energy. We also confirmed numerically within the variational wave functions (12) and (13) that the ground state is always singlet and thus the transition to the triplet state does not take place as a consequence of the Kondo effect. Such a smooth crossover at zero temperature is in contrast to the polaron-molecule transition in the corresponding impurity problem without the confinement potential which was found both for s -wave and p -wave Feshbach resonances [34, 35]. We finally note that the spectral density function of the impurity B atom is obtained from $\rho_B(\omega) = -\frac{1}{\pi} \text{Im} G(\omega + i0^+)$, which exhibits a δ -function peak at $\omega = E_s$ and a continuum above $\omega = E_t$. This quantity can be measured in ultracold atom experiments with the radio-frequency spectroscopy [36–38], and, accordingly, the binding energy of the Kondo singlet (16) as well.

Concluding remarks

In this Letter, we proposed and elaborated a simple but novel scheme to realize the $\text{SU}(3)$ orbital Kondo effect with ultracold atoms. In addition to its simplicity, the advantage of our system (1) also lies in its versatility. For example, by deforming the isotropic confinement potential $V_B(r)$, the p -orbital degeneracy can be reduced from threefold to twofold, which now leads to an $\text{SU}(2)$ orbital Kondo effect. Moreover, by further increasing the interspecies attraction U_{AB} , an ℓ th partial-wave scattering resonance can be induced [22], where an $\text{SU}(2\ell + 1)$ orbital Kondo effect will emerge in the same

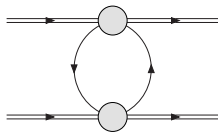


FIG. 3. Leading interdimer interaction mediated by a surrounding Fermi sea of spinless fermions. See Fig. 1 for the meanings of the symbols.

system (1). The Kondo effect thus realized in our scheme causes a logarithmic growth of the atom-dimer scattering rate, which may be observed in ultracold atom experiments as an increasing atom loss by lowering the temperature. This hallmark is a direct analog of the celebrated increasing electrical resistivity in dilute magnetic alloys [3, 33]. Moreover, the spectral density function of the Kondo singlet and its binding energy can be measured in our scheme with the radio-frequency spectroscopy, which will be useful to develop further insights into the Kondo physics.

Our scheme can be easily extended to a dense Kondo lattice where localized impurities are placed periodically and a competition between the Kondo effect and the Ruderman-Kittel-Kasuya-Yosida (RKKY) interaction is expected to lead to a rich phase diagram with a quantum critical point [2, 39]. In particular, the RKKY interaction in our system is unusual because orbital indices of localized impurities are correlated with a direction in which they are separated [30]. This feature can be seen by considering two bound dimers localized at \mathbf{r} and \mathbf{r}' with a separation $\mathbf{r} - \mathbf{r}' = R\hat{z}$ chosen in the z direction. Here surrounding spinless fermions mediate an effective interaction between the two localized dimers, which can be computed from the atom-dimer Hamiltonian (7) in a perturbative expansion over $a_p k_F^3 \ll 1$. The leading $O(a_p^2)$ term is depicted in Fig. 3, which at a large separation $k_F R \gg 1$ is found to be universal, i.e., independent of the cutoff Λ' , and given by

$$H_{\text{RKKY}} = \frac{9a_p^2 k_F^5 \cos(2k_F R)}{2\pi m_A R^3} \phi_z^\dagger(\mathbf{r}) \phi_z(\mathbf{r}) \phi_z^\dagger(\mathbf{r}') \phi_z(\mathbf{r}') + O(R^{-4}) + O(a_p^3), \quad (17)$$

where p -orbital indices of the localized dimers are locked to the direction of their separation. Because of the geometrical frustration, such a strongly anisotropic interdimer interaction may lead to an interesting many-body physics of the dense Kondo lattice realized in our scheme, which is to be studied in the future.

[1] A. C. Hewson, *The Kondo Problem to Heavy Fermions* (Cambridge University Press, Cambridge, England, 1993).

- [2] P. Coleman, in *Handbook of Magnetism and Advanced Magnetic Materials*, edited by H. Kronmüller and S. Parkin (John Wiley & Sons, New York, 2007).
- [3] J. Kondo, Prog. Theor. Phys. **32**, 37 (1964).
- [4] D. Goldhaber-Gordon, H. Shtrikman, D. Mahalu, D. Abusch-Magder, U. Meirav, and M. A. Kastner, Nature (London) **391**, 156 (1998).
- [5] S. M. Cronenwett, T. H. Oosterkamp, and L. P. Kouwenhoven, Science **281**, 540 (1998).
- [6] J. Schmid, J. Weis, K. Eberl, and K. von Klitzing, Physica (Amsterdam) B **256–258**, 182 (1998).
- [7] J. Nygård, D. H. Cobden, and P. E. Lindelof, Nature (London) **408**, 342 (2000).
- [8] M. R. Buitelaar, A. Bachtold, T. Nussbaumer, M. Iqbal, and C. Schönenberger, Phys. Rev. Lett. **88**, 156801 (2002).
- [9] J. Park, A. N. Pasupathy, J. I. Goldsmith, C. Chang, Y. Yaish, J. R. Petta, M. Rinkoski, J. P. Sethna, H. D. Abruña, P. L. McEuen, and D. C. Ralph, Nature (London) **417**, 722 (2002).
- [10] W. Liang, M. P. Shores, M. Bockrath, J. R. Long, and H. Park, Nature (London) **417**, 725 (2002).
- [11] D. L. Cox and A. Zawadowski, Adv. Phys. **47**, 599 (1998).
- [12] O. Yu. Kolesnychenko, R. de Kort, M. I. Katsnelson, A. I. Lichtenstein, and H. van Kempen, Nature (London) **415**, 507 (2002).
- [13] P. Jarillo-Herrero, J. Kong, H. S. J. van der Zant, C. Dekker, L. P. Kouwenhoven, and S. De Franceschi, Nature (London) **434**, 484 (2005).
- [14] L. Kouwenhoven and L. Glazman, Phys. World **14**, 33 (2001).
- [15] I. Bloch, J. Dalibard, and S. Nascimbène, Nat. Phys. **8**, 267 (2012).
- [16] A. Recati, P. O. Fedichev, W. Zwerger, J. von Delft, and P. Zoller, arXiv:cond-mat/0212413.
- [17] G. M. Falco, R. A. Duine, and H. T. C. Stoof, Phys. Rev. Lett. **92**, 140402 (2004).
- [18] B. Paredes, C. Tejedor, and J. I. Cirac, Phys. Rev. A **71**, 063608 (2005).
- [19] L.-M. Duan, Europhys. Lett. **67**, 721 (2004).
- [20] A. V. Gorshkov, M. Hermele, V. Gurarie, C. Xu, P. S. Julienne, J. Ye, P. Zoller, E. Demler, M. D. Lukin, and A. M. Rey, Nat. Phys. **6**, 289 (2010).
- [21] S. Lal, S. Gopalakrishnan, and P. M. Goldbart, Phys. Rev. B **81**, 245314 (2010).
- [22] Y. Nishida and S. Tan, Phys. Rev. A **82**, 062713 (2010).
- [23] G. Lamporesi, J. Catani, G. Barontini, Y. Nishida, M. Inguscio, and F. Minardi, Phys. Rev. Lett. **104**, 153202 (2010).
- [24] P. Massignan and Y. Castin, Phys. Rev. A **74**, 013616 (2006).
- [25] S. E. Barnes, J. Phys. F **6**, 1375 (1976); **7**, 2637 (1977).
- [26] P. Coleman, Phys. Rev. B **29**, 3035 (1984).
- [27] V. Gurarie and L. Radzihovsky, Ann. Phys. (Amsterdam) **322**, 2 (2007).
- [28] M. Jona-Lasinio, L. Pricoupenko, and Y. Castin, Phys. Rev. A **77**, 043611 (2008).
- [29] J. R. Schrieffer and P. A. Wolff, Phys. Rev. **149**, 491 (1966).
- [30] B. Coqblin and J. R. Schrieffer, Phys. Rev. **185**, 847 (1969).
- [31] T. Köhler, K. Góral, and P. S. Julienne, Rev. Mod. Phys. **78**, 1311 (2006).
- [32] C. Chin, R. Grimm, P. Julienne, and E. Tiesinga, Rev.

- Mod. Phys. **82**, 1225 (2010).
- [33] W. J. de Haas, J. de Boer, and G. J. van den Berg, *Physica (Amsterdam)* **1**, 1115 (1934).
- [34] F. Chevy and C. Mora, *Rep. Prog. Phys.* **73**, 112401 (2010).
- [35] J. Levinsen, P. Massignan, F. Chevy, and C. Lobo, *Phys. Rev. Lett.* **109**, 075302 (2012).
- [36] A. Schirotzek, C.-H. Wu, A. Sommer, and M. W. Zwierlein, *Phys. Rev. Lett.* **102**, 230402 (2009).
- [37] C. Kohstall, M. Zaccanti, M. Jag, A. Trenkwalder, P. Massignan, G. M. Bruun, F. Schreck, and R. Grimm, *Nature (London)* **485**, 615 (2012).
- [38] M. Knap, A. Shashi, Y. Nishida, A. Imambekov, D. A. Abanin, and E. Demler, *Phys. Rev. X* **2**, 041020 (2012).
- [39] Q. Si and F. Steglich, *Science* **329**, 1161 (2010).